REVIEW

Check for updates

Recent progress in the shape deformation of polymeric hydrogels from memory to actuation

Baoyi Wu,[ab] Huanhuan Lu,[ab] Xiaoxia Le,[ab] Wei Lu, [ID] [ab] Jiawei Zhang, [ID] *[ab] Patrick Théato [ID] [cd] and Tao Chen [ID] *[ab]

Shape deformation hydrogels, which are one of the most promising and essential classes of stimuli-responsive polymers, could provide large-scale and reversible deformation under external stimuli. Due to their wet and soft properties, shape deformation hydrogels are anticipated to be a candidate for the exploration of biomimetic materials, and have shown various potential applications in many fields. Here, an overview of the mechanisms of shape deformation hydrogels and methods for their preparation is presented. Some innovative and efficient strategies to fabricate programmable deformation hydrogels are then introduced. Moreover, successful explorations of their potential applications, including information encryption, soft robots and bionomic systems, are discussed. Finally, remaining great challenges including the achievement of multiple stable deformation states and the combination of shape deformation and sensing are highlighted.

1. Introduction

Nature has been regarded as a source of inspiration for the development of artificial intelligent materials.[1–3] For example,

[a]Key Laboratory of Marine Materials and Related Technologies, Zhejiang Key Laboratory of Marine Materials and Protective Technologies, Ningbo Institute of Material Technology and Engineering, Chinese Academy of Sciences, Ningbo, 315201, China. E-mail: zhangjiawei@nimte.ac.cn; tao.chen@nimte.ac.cn

[b]School of Chemical Sciences, University of Chinese Academy of Sciences, 19A Yuquan Road, Beijing 100049, China

[c]Soft Matter Synthesis Laboratory, Institute for Biological Interfaces IIII, Karlsruhe Institute of Technology (KIT), Hermann-von-Helmholtz-Platz 1, D-76344 Eggenstein-Leopoldshafen, Germany

[d]Institute for Chemical Technology and Polymer Chemistry, Karlsruhe Institute of Technology (KIT), Enge Sser Str. 18, D-76131 Karlsruhe, Germany

biological organisms are able to adjust their shape to accommodate to a variety of environmental demands and external perturbations such as escape and predation. Similarly, shape transformation hydrogels, which are one of the most promising classes of bionic intelligent materials, can translate various external stimuli such as pH,[4–6] heat,[7–9] ionic strength[10–12] and light[13–15] into controllable and reversible deformation. Compared with other shape deformation materials such as shape memory alloys[16] and liquid crystalline actuators,[17] shape transformation hydrogels can provide larger-scale deformation due to their soft and wet properties.[18,19] Therefore, shape deformation hydrogels have attracted tremendous attention and shown potential applications in soft robots,[20,21] biomimetic devices[22,23] and intelligent valves.[24,25]

Baoyi Wu received his MS from Shanghai University, China, in 2020. Currently, he is a PhD student at the Ningbo Institute of Materials Technology and Engineering, Chinese Academy of Sciences, under the supervision of Prof. Jiawei Zhang and Prof. Tao Chen. His research interests are focused on intelligent deformable hydrogels and their applications.

Prof. Jiawei Zhang received her Ph.D. in Polymer Chemistry and Physics from Nankai University in 2010. After postdoctoral training at Tsinghua University, China, she joined the Ningbo Institute of Materials Technology and Engineering, Chinese Academy of Sciences, as an Associate Professor in 2013. She was promoted to Full Professor in 2017. Her research interests are focused on intelligent deformable polymers including shape memory polymers and polymeric actuators.

Shape deformation hydrogels can be divided into two types based on the shape deformation direction. The first type comprises hydrogels that transform to a known state. A shape memory hydrogel is first deformed into a temporary shape by an external force and fixed. Then, through the shape recovery process, the temporary shape can self-deform into the known original shape.[26–28] The second type is hydrogels that transform to an unknown state. A hydrogel actuator can self-deform into an unknown shape determined by its structure *via* the local swelling/de-swelling of the hydrogel networks.[29,30] In past years, shape memory hydrogels and actuating hydrogels have been considered to be two independent concepts, and corresponding reviews of both have been published.[31–34] However, with the rapid development of this field, especially in the last five years, many innovative strategies to provide programmable shape deformation by combining shape memory and actuation behavior have been proposed, and some attractive applications such as soft robots and information encryption have been exhibited, expanding their potential applications (Fig. 1). Thus, we feel that it is highly necessary and important to summarize the notable progress in shape deformation hydrogels and discuss their future perspectives. In this review, the mechanism of traditional shape deformation hydrogels, including shape memory hydrogels and actuating hydrogels, will be briefly described first. The fabrication of programmable shape deformation hydrogels *via* the synergy of shape memory and actuation will then be discussed, followed by some novel potential applications. Finally, we will give perspectives regarding both current challenges and future development directions.

2. Mechanism of shape transformation hydrogels

Shape memory hydrogels with excellent shape encoding properties and hydrogel actuators with reversible shape deformation behavior are the two main categories of shape deformation hydrogels.

Prof. Tao Chen received his Ph.D. in Polymer Chemistry and Physics from Zhejiang University in 2006. After his postdoctoral training at the University of Warwick, he joined Duke University as a research scientist. He then moved back to Europe as an Alexander von Humboldt Research Fellow at Technische Universität Dresden, Germany. Since 2012, he has been a full-time professor at the Ningbo Institute of Materials Technology and Engineering, Chinese Academy of Sciences. His research interests include smart polymeric materials and their hybrid systems with applications in actuators, shape memory polymers, and chemical sensing.

2.1 Shape-memory-induced shape deformation

Shape memory hydrogels are capable of being fixed into temporary shapes *via* the formation of reversible crosslinks and provide programmable shape deformation in the shape recovery process.

Since the temporary shape of the first shape memory hydrogel was fixed *via* crystalline aggregates,[35] diverse interactions have been introduced into hydrogel networks to expand this field, such as hydrogen bonds,[36,37] metal–ligand coordination,[38,39] host–guest interactions,[40,41] boronate ester bonds[42,43] and Schiff base bonds (Fig. 2). For example, a straight polyacrylamide/alginate (PAAm/Alg) hydrogel strip can be shaped into a circle by an external force and then immersed in a $CaCl_2$ solution in order to fix the temporary shape *via* Ca^{2+}–Alg coordination. The shape deformation process can occur in an ethylene diamine tetraacetic acid (EDTA) solution, in which the circle will transform into a straight strip because the Ca^{2+} will be extracted by EDTA, and the Ca^{2+}–Alg crosslinks will be disassembled. Since the hydrogel can be fixed into a variety of temporary shapes while the original shape is predetermined, shape memory hydrogels can realize shape transformation from various temporary shapes into the known original shape.

2.2 Actuation-induced shape deformation

Another class of materials that can accomplish shape transformation is hydrogel actuators, which exhibit reversible shape transformation *via* the local swelling/de-swelling of stimuli-responsive hydrogels under external stimuli such as pH, heat, light, or ionic strength. Due to their isotropic structure, traditional hydrogel actuators can only achieve simple homogeneous swelling/shrinking. In order to realize complex actuation behavior and further expand the applications of hydrogel actuators, diverse anisotropic structures such as bilayer structures,[44,45] gradient structures,[46–48] patterned structures,[49,50] and oriented structures[51,52] have been explored. Taking bilayer structures as an example, bilayer hydrogel actuators usually consist of two hydrogel sheets: one called the active layer and another called the passive layer. The active layer can provide reversible swelling/de-swelling in response to stimuli while the passive layer cannot. In this way, the bilayer hydrogel actuator bends toward the passive layer when the active layer swells and toward the actuating layer when the active layer de-swells (Fig. 3).

Recently, in order to overcome the unexpected swelling of the passive layer, non-swelling materials such as poly-dimethylsiloxane (PDMS) and paper[53,54] have been explored as passive layers to fabricate bilayer hydrogel actuators. For instance, Gong and coworkers used glass fiber (GF) fabrics to combine tough polyampholyte hydrogels with PDMS and prepared a bilayer hydrogel actuator that demonstrated solvent-responsive behavior in acetone.[53] Additionally, Zhou and coworkers proposed a novel strategy to fabricate a poly-dimethylsiloxane/poly(*N*-isopropylacrylamide)-poly(acrylic acid) (PDMS/PNIPAm-PAA) bilayer hydrogel actuator *via* surface catalytically initiated radical polymerization (SCIRP).[54] Compared to the preparation of PDMS/hydrogel bilayer
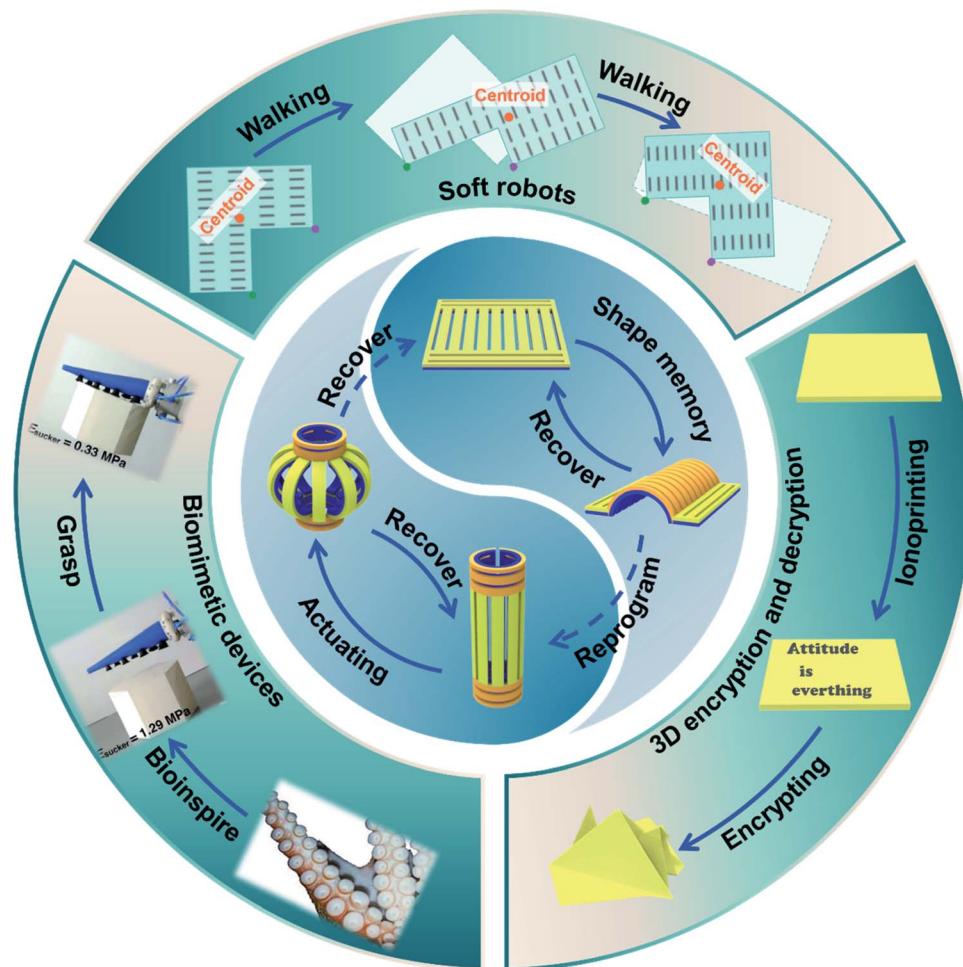
Fig. 1 An overview of the types of shape deformation hydrogels and their potential applications. (Center) Reproduced with permission from ref. 88. Copyright 2020 Wiley-VCH. (Top) Reproduced with permission from ref. 51. Copyright 2015 Nature Publishing Group. (Left) Reproduced with permission from ref. 97. Copyright 2020 AAAS. (Right) Reproduced with permission from ref. 103. Copyright 2019 Wiley-VCH.
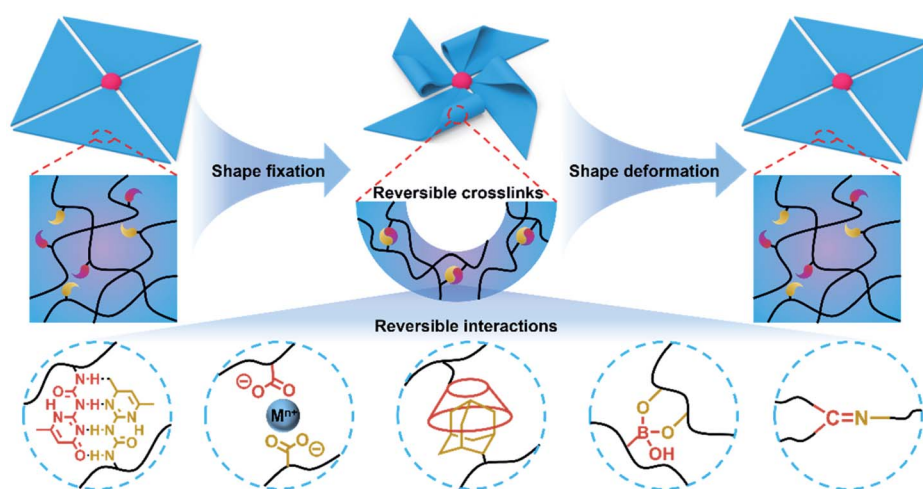

Fig. 2 Schematic illustration showing the deformation mechanism of shape memory hydrogels.

hydrogel actuators, the preparation of a bilayer hydrogel on a hydrophilic surface such as paper can be easier. In our previous work, pan paper was employed as a passive layer. The hydrogel precursor was poured onto the surface of the pan paper and slightly penetrated the hydrophilic pan paper to form a bilayer hydrogel actuator.[55]
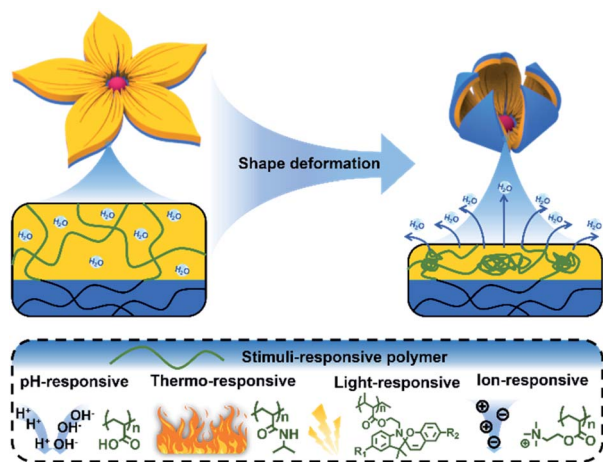
Fig. 3 Schematic illustration showing the deformation mechanism of an actuating hydrogel.

It is worth noting that when some stimulus-responsive materials such as magnetic particles or free ions are added to a hydrogel network, even a non-responsive hydrogel can provide shape transformation.[56,57] For example, Lee and coworkers fabricated an electro-active hydrogel (EAH) actuator consisting of acrylic acid (AA) as a monomer, which could self-deform under an electric field.[56] According to the Flory theory and Donnan equilibrium, the carboxylic groups in the EAH network will be ionized and generate a large number of mobile cations under an electric field. Due to the directional movement of the mobile cations, osmotic pressure develops and induces the shape deformation of the EAH. With the diverse design possibilities in terms of both the anisotropic structure and selection of materials, hydrogel actuators will continue to provide new fascinating shape deformations in the future.

3. Programming the shape transformation of shape memory hydrogels

As mentioned above, shape memory hydrogels can be fixed into various temporary shapes *via* the formation of reversible crosslinks, which means that diverse shapes can be encoded into the hydrogels and the corresponding programmed shape transformation can be achieved by the shape recovery process. In this section, we will discuss the design principles and programmable transformation performance of shape memory hydrogels.

3.1 Shape memory hydrogels with one-step shape deformation

Initially, only one kind of reversible crosslink was introduced in shape memory hydrogel networks, which meant that only one temporary shape could be stabilized in one shape memory process, and that the shape memory hydrogel would exhibit only one-step deformation from the temporary shape to the original shape in response to an external stimulus. For example,

in our previous work, dynamic phenylboronic acid (PBA)–diol interactions were applied to fix the temporary shape.[41] The original straight hydrogel strip could be fixed into a temporary shape such as a circle under alkaline conditions *via* the generation of PBA–diol ester bonds, and shape deformation could be triggered by acidic conditions or aqueous solutions of glucose and fructose.

Recently, Wu and coworkers prepared a photo-responsive shape memory hydrogel that exhibits programmable deformation behavior under NIR irradiation.[58] Gold nanorods (AuNRs) were incorporated into a poly(methacrylic acid-*co*-methacrylamide) hydrogel (P(MAAm-*co*-MAAc)) after being stabilized by methoxy polyethylene glycol thiol (MPEG-SH) (Fig. 4a). The P(MAAm-*co*-MAAc) hydrogel exhibited excellent thermo-responsive behavior, and the tensile breaking stress of the P(MAAm-*co*-MAAc) hydrogel decreased from 16 MPa to 2 MPa when the test temperature was increased from 4 to 70 °C (Fig. 4b). This indicated that the P(MAAm-*co*-MAAc) hydrogel can be shaped at high temperature and fixed into a temporary shape at low temperature. Due to the photothermal effect of the AuNRs, the local temperature in the P(MAAm-*co*-MAAc) hydrogel can reach ~60 °C within 10 s of irradiation with NIR light (I_{NIR} of 467 mW mm^{-2}) (Fig. 4c). Based on the excellent photothermal effect of the AuNRs and thermo-responsive shape memory behavior of the P(MAAm-*co*-MAAc) hydrogel, a programmable deformation process was demonstrated. First, the P(MAAm-*co*-MAAc) hydrogel was prestressed and fixed in the temporary shape. The P(MAAm-*co*-MAAc) hydrogel was then irradiated with NIR light. Due to light absorption, the photothermal efficiency was different at the upper and bottom layers of the light-exposed region. The temperature of the upper layer may increase more rapidly than that of the bottom layer; thus, the upper layer may recover its original shape, while the bottom layer does not. This anisotropic recovery behavior induced folding deformation. Using a 1D hydrogel strip, programmable deformation to form various shapes, such as "0", "2", "6", "7", "8" and "M" shapes, was demonstrated by controlling the irradiation position (Fig. 4d). Additionally, a 2D square hydrogel with four legs could be programmed in the same way and deformed into various 3D shapes (Fig. 4e).

3.2 Shape memory hydrogels with multi-step shape deformation

As mentioned above, shape memory hydrogels could only provide one-step shape deformation initially, which limited their potential applications, thus arousing increasing interest in the exploration of shape memory hydrogels with multi-step shape deformation, or in other words, hydrogels that can be fixed into two or more temporary shapes in one shape memory process.[5,59,60] There are two main strategies for the fabrication of shape memory hydrogels with multi-step shape deformation: (1) incorporating two or more non-interfering molecular switches into one hydrogel system and (2) applying reversible crosslinking with a broad transition range. For instance, three non-interfering switchable interactions, namely, metal coordination, reversible PBA–diol ester bonds, and the coil-helix
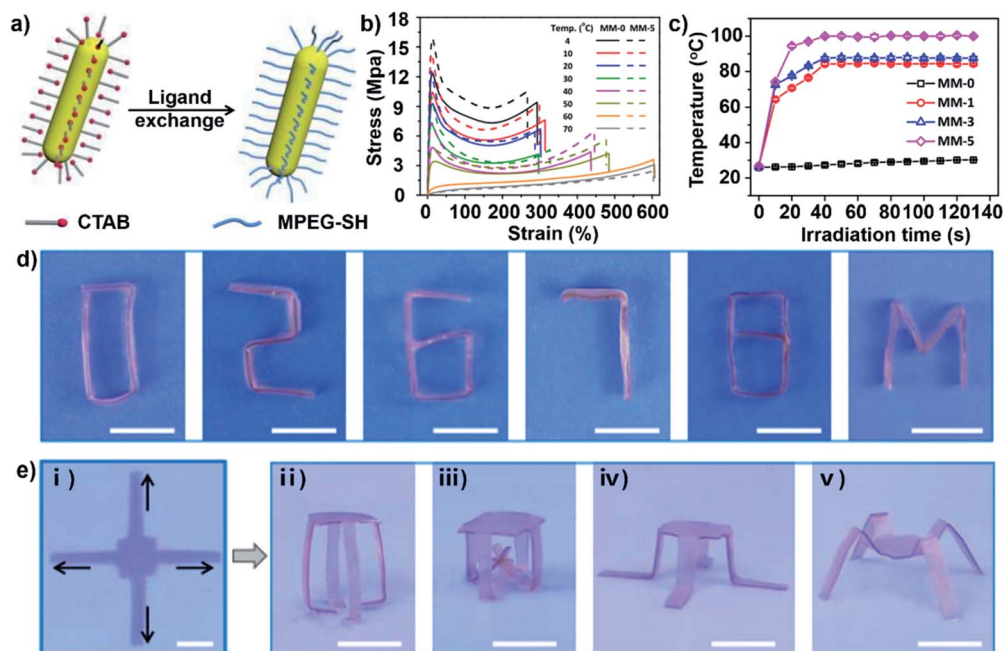
Fig. 4 (a) Schematic of the ligand exchange of AuNRs. (b) Tensile stress–strain curves of the P(MAAm-*co*-MAAc) hydrogel. (c) Photo-thermo behavior of the P(MAAm-*co*-MAAc) hydrogel with different concentrations of AuNRs. (d) Various programmable deformations of hydrogel strips. (e) Various programmable deformations of hydrogel sheets. Scale bars: 1 cm. Reproduced with permission from ref. 58. Copyright 2019 American Chemical Society.
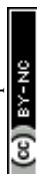
transition of agar, were incorporated to prepare a shape memory hydrogel with a multi-step shape deformation effect.[5] Three different temporary shapes could be established by the formation of the three reversible crosslinks in turn. The hydrogel was first bent by an external force in 60 °C water and then fixed in temporary shape I at 4 °C *via* the formation of the helix structure of agar. The hydrogel was then shaped again and immersed in a Gly–NaOH buffer solution (pH = 10.6) to fix it in temporary shape II *via* the generation of PBA–diol ester bonds. Finally, the hydrogel was shaped into a "W" shape and fixed in temporary shape III *via* the coordination of Fe^{3+} and carboxylic groups. The deformation from temporary shape III to temporary shape II was realized by immersing the hydrogel in a competitive ligand (EDTA) solution, and the hydrogel was deformed from temporary shape II into temporary shape I by immersing it in HCl solution to destroy the PBA–diol ester bonds. Finally, it was transformed from temporary shape I to the original shape in a warm environment as agar returned to the coil state.

Recently, another strategy has been explored to prepare shape memory hydrogels with multi-step shape deformation by employing reversible crosslinking with a broad transition range.[61,62] Gao and coworkers modified polyvinyl alcohol (PVA) with single-component octyl chains and prepared multiple shape memory hydrogels by a water–vapor exchange process.[59] Due to the random dispersion of the single-component octyl chains on the PVA chain, clusters were formed with different numbers of alkyl side chains. These broadly dispersed clusters served as switchable crosslinking points to orthotopically offer multiple temporary shapes and editable permanent shapes, respectively (Fig. 5a). Therefore, the shape memory process

could be induced by the sequential thermal dissociation of the weak and strong hydrophobic clusters from T_1 (low temperature) to T_n (high temperature). For example, the hydrogel was first heated to 90 °C (Fig. 5c). The hydrogel was then stretched to 300% strain, and temporary shape I was fixed by cooling the temperature to 60 °C. The hydrogel was then further stretched to 500% strain and temporary shape II was fixed at 20 °C. Finally, all of the temporary shapes were recovered as the temperature gradually rose to 60 °C. In order to vividly demonstrate the shape memory and shape deformation process, a square hydrogel film was folded into a three-dimensional (3D) permanent tortoise. The origami structure could subsequently be programmed into various temporary shapes, such as flat and dome shapes, at different temperatures. When the temperature was increased, the temporary shapes could spontaneously deform to the permanent shape (Fig. 5d). In addition to distinct thermal transitions, the assembly of chitosan chains into microcrystals under alkaline conditions and chain entanglement in NaCl solution were also applied to construct shape memory hydrogels with multi-step shape deformation behavior.[63] These successful attempts may open up a vast array of approaches in both the design and programmability of shape memory hydrogels.

4. Programming the shape transformation of hydrogel actuators

Since the anisotropic structure of traditional hydrogel actuators is distributed in the horizontal or vertical direction, traditional
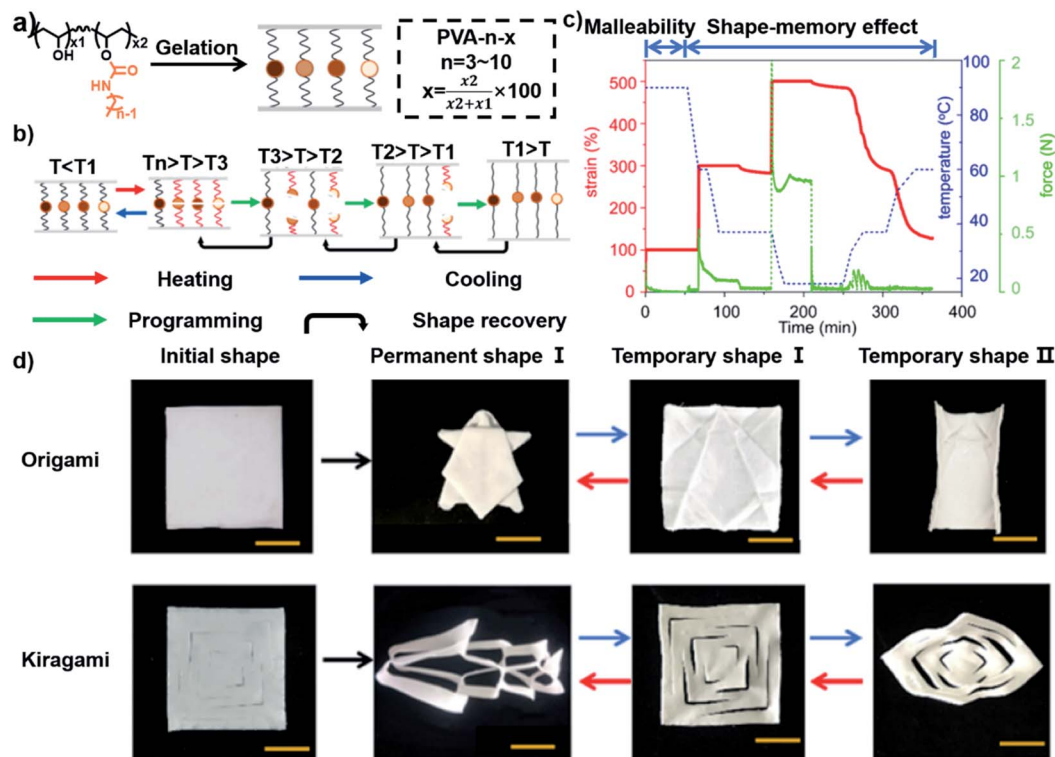
Fig. 5 (a) Schematic illustration showing the structure of short alkyl side chain modified PVA. (b) Schematic illustration showing the mechanism of a multiple-shape memory process. (c) Thermal cycle of the shape memory and recovery process. (d) Images showing the programmable shape deformation of origami and kirigami structures. Scale bars: 2 mm. Reproduced with permission from ref. 59. Copyright 2019 American Chemical Society.

hydrogel actuators can only exhibit simple deformation behaviors such as bending. Recently, an increasing number of strategies have been explored to simultaneously construct anisotropy in both the horizontal and vertical directions of the hydrogel actuator during or after the fabrication process, enabling the programmable deformation of hydrogel actuators and more complex deformation behavior. In this section we will describe a series of design principles and the transformation performances of hydrogel actuators.

4.1 Anisotropy produced during fabrication

It is a universal principle that the anisotropic actuation behavior is determined by the heterogeneous structures of hydrogels, such as bilayer structures, gradient structures, patterned structures, and oriented structures. The anisotropic structure of an actuating hydrogel is normally encoded during the fabrication process.[64–67] For example, Yum and coworkers prepared a temperature-responsive hydrogel with a continuously varied composition using digital light 4D printing (Fig. 6a).[68] The hydrogel precursor was exposed to digital light, and the anisotropic structure was generated by controlling the light exposure time (t_{ex}). The density of the network increased with increasing t_{ex}, and the increase in the density in turn reduced the degree and rate of macroscopic swelling and shrinking. In this way, a 2D hydrogel disc could be pre-programmed and deformed into various complex 3D morphologies (Fig. 6b). Similarly, Wu and coworkers combined

a high-swelling hydrogel strip with a non-swelling hydrogel plane using multistep photolithographic polymerization.[69] Due to the confinement of the frame, the swelling hydrogel strips
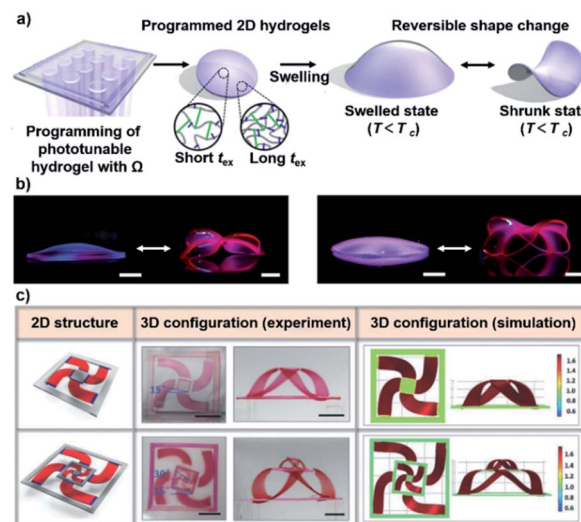

Fig. 6 (a) Schematic illustration showing the programming and deformation process of the phototunable hydrogels. (b) Images showing the deformation of the complex from 2D to 3D *via* isotropic swelling. Scale bars: 2 mm. Reproduced with permission from ref. 68. Copyright 2018 Nature Publishing Group. (c) Programmable deformation with localized rotation from 2D to 3D. Scale bars: 1 cm. Reproduced with permission from ref. 69. Copyright 2020 Wiley-VCH.

buckled out of the plane in order to release the internal stress, which induced a deformation from a 2D to a 3D structure. As shown in Fig. 6c, inspired by the kirigami structure, a high-swelling hydrogel could be grown on the non-swelling hydrogel plane in a patterned fashion to provide a variety of programmed deformations.

In addition, the anisotropic structure of actuating hydrogels can also be endowed with and coded by electrostatic repulsion during the fabrication process.[21,51,52,70,71] For example, Aida and coworkers developed an innovative actuating hydrogel with oriented electrolyte nanosheets.[51] The actuating hydrogel was polymerized from a NIPAm hydrogel precursor and contained titanate(IV) nanosheets (TiNSs). The TiNSs could be oriented and aligned orthogonally to the applied flux lines of a magnetic field, and the resulting actuating hydrogel exhibited orientated actuating behavior at 45 °C. Similarly, Wu and coworkers used fluorohectorite $[Na_{0.5}][Li_{0.5}Mg_{2.5}][Si_4]O_{10}F_2$ nanosheets to fabricate an anisotropic hydrogel in an electric field (Fig. 7a).[71] The rectangular samples exhibited anisotropic deformation with expansion perpendicular to the alignment of the nanosheets and contraction parallel to the alignment of the nanosheets (Fig. 7b). Moreover, when the electric field was encoded, the corresponding dispersion of NSs was formed. As shown in Fig. 7c, the anisotropic hydrogel could exhibit programmable deformation from a disc to a saddle-shaped configuration at 37 °C. In order to better control the programmable deformation, gold nanoparticles (AuNPs) were utilized to provide high photothermal conversion efficiency so that the hydrogel would self-deform under NIR irradiation. As shown in Fig. 7d, a ring-shaped hydrogel was programmed using a pair of circular electrodes to form radially oriented nanosheets, and the ring-shaped hydrogel was locally irradiated with a NIR laser beam in order to induce the deformation from a ring shape to a saddle shape. More interestingly, when the laser beam was scanned along the ring shape, the ring-shaped hydrogel moved continuously due to the constant change in the barycenter of the ring-shaped hydrogel. These works made an essential exploration of the programmability of the anisotropic structures of actuating hydrogels and provided innovative strategies to produce sophisticated locomotion.

4.2 Anisotropy produced after fabrication

The anisotropy of traditional hydrogel actuators is usually stable and irreversible, making it difficult to reprogram the deformation behavior of the hydrogel actuators after the fabrication process. Inspired by Lego assembly, Xie and coworkers proposed a highly versatile modular approach to construct a reprogrammable hydrogel actuator.[72] As shown in Fig. 8a, first, a responsive host hydrogel (RH) containing both β-CD (host groups) and carboxylic acid (responsive unit) and a non-responsive guest hydrogel (NRG hydrogel) containing only ferrocene guest units (with no carboxylic acid) were prepared, respectively. Strips of RH and NRG were then manually pushed together to form a bilayer hydrogel actuator via the host–guest interaction between the β-CD and ferrocene moieties. The bilayer hydrogel strip could bend spontaneously when triggered by pH and ionic strength (Fig. 8b). It is worth noting that the bilayer could be rejoined even after being cut into two halves and deformed into an "S" shape (Fig. 8c). Recently, in order to enhance the interfacial interaction, we used dynamic boronic ester bonds to connect two different bulk hydrogels containing
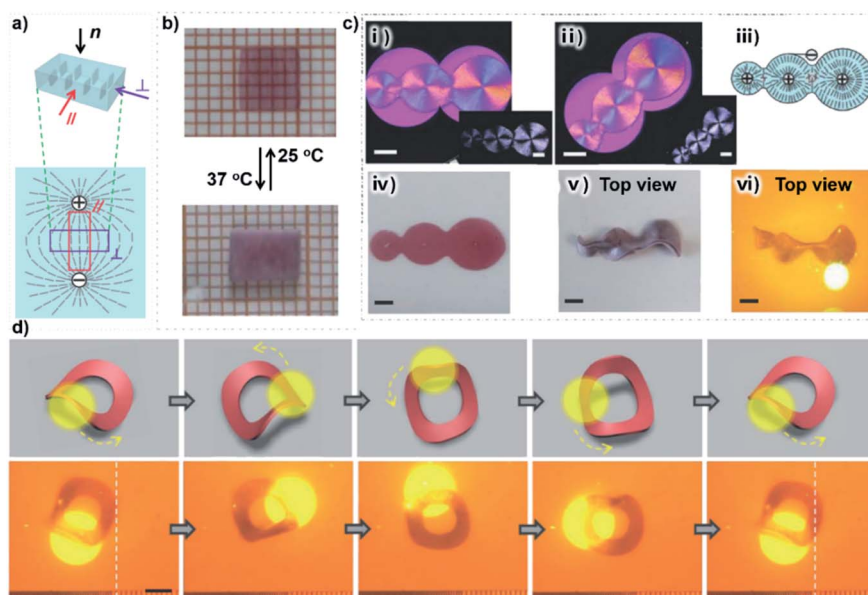

Fig. 7 (a) Schematic illustration showing the alignment of the nanosheets in the composite hydrogel. (b) Images showing the anisotropic actuating behavior of a hydrogel sheet. (c) Images showing the programmed hydrogel with a radial nanosheet orientation and its programmable deformation in hot water or upon NIR irradiation. (d) Images showing the programmed-deformation-induced sophisticated locomotion process of a ring-shaped hydrogel via programmable deformation with localized rotation from 2D to 3D. Scale bars: 5 mm. Reproduced with permission from ref. 71. Copyright 2020 Wiley-VCH.
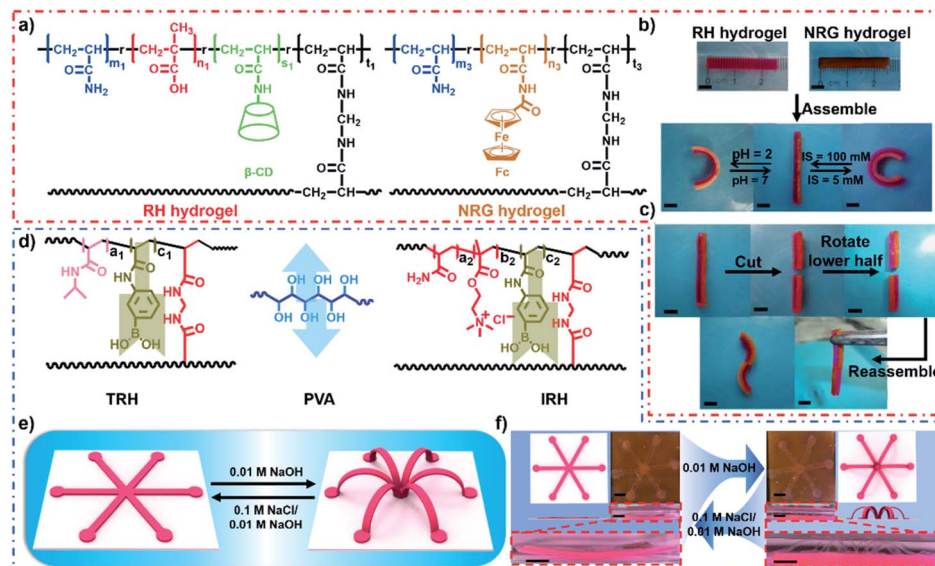
Fig. 8 (a) Chemical structures of a RH and NRG hydrogel. (b) Reversible deformation behavior of a modular assembly hydrogel. (c) Self-healing and deformation behavior of a modular assembly hydrogel. Scale bars: 5 mm. Reproduced with permission from ref. 72. Copyright 2015 Wiley-VCH. (d) Modular assembly process of the bilayer: PVA is utilized as a supramolecular glue to assemble two hydrogels with phenylboronic acid groups. (e and f) Programmable 2D-to-3D deformation process. Scale bars: 1 cm.

phenylboronic acid groups *via* poly (vinyl alcohol) (PVA) (Fig. 8d).[73] When the assembled hydrogel was stretched, the assembled position remained intact even if the hydrogel body broke. Furthermore, as shown in Fig. 8e and f, the central and end parts of an "octopus"-shaped ionic-strength-responsive hydrogel were assembled into a non-responsive hydrogel sheet, thereby providing programmable 2D-to-3D deformation as the ionic strength was decreased.

In addition to modular assembly, ionoprinting can also be utilized to program the deformation behavior of hydrogel actuators after the fabrication process.[74–77] Metal ions are patterned on the surface of hydrogel and coordinate with the carboxyl groups of the hydrogel network, which changes the local crosslink density. Due to the horizontal anisotropy of the pattern and the vertical anisotropy of the crosslink gradient, the hydrogel sheet can exhibit various programmed deformations. For instance, Fu and coworkers placed an iron electrode on the surface of a P(NIPAM-*co*-NaMAc) hydrogel. A density gradient was generated by the diffusion of Fe^{3+} and induced heterogeneous shrinkage of the hydrogel actuator.[74] Furthermore, more complex patterns could be printed and the programmed deformation was applied to produce an intelligent hydrogel gripper. Similarly, Wang and coworkers utilized an Fe^{3+} solution as an ink and printed various patterns onto the surface of a poly(sodium acrylate) hydrogel *via* a facile and versatile computer-assisted ion inkjet printing technique.[75] Through changing the printing times or the different/gradient grayscale distribution of the designed patterns, various programmed deformations could be achieved. These works provided complex and precise programmable deformations, which may prove an essential step to reprogram the deformation behavior after the fabrication process.

4.3 Anisotropy produced by 3D printing

Recently, 3D printing has attracted increasing attention since it has no obvious restrictions in the fabrication of hydrogels with complex 3D morphologies.[78–82] Additionally, hydrogel actuators with anisotropic structures can be obtained by 3D printing and
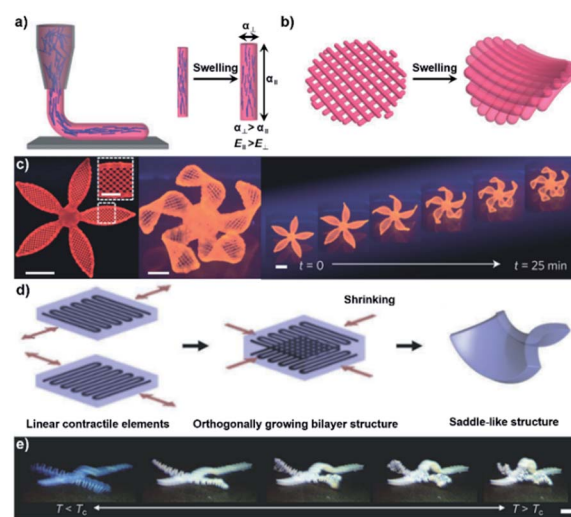

Fig. 9 (a) Schematic illustration showing the 3D printing process with oriented NFC. (b) Isotropic swelling behavior of the 3D printed hydrogel. (c) Bionomic programmable deformation of the 3D printed flower-shaped hydrogel. Scale bars: 5 mm, inset = 2.5 mm. Reproduced with permission from ref. 83. Copyright 2016 Nature Publishing Group. (d) Schematic illustration showing a bilayer hydrogel obtained by 3D printing. (e) Programmable and multi-mode deformation of the 3D printed hydrogel. Scale bars: 5 mm. Reproduced with permission from ref. 84. Copyright 2018 Wiley-VCH.
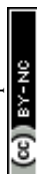
exhibit programmable 4D shape deformation.[83–86] For instance, when a viscoelastic ink containing nanofibrillated cellulose (NFC) was printed, the NFCs could be oriented to provide anisotropic swelling behavior *via* the shear orientation of the nozzle (Fig. 9a and b).[83]

On this basis, Lewis and coworkers encoded localized swelling anisotropy during the printing process and obtained a biomimetic hydrogel with programmable 4D shape deformation. As shown in Fig. 9c, a flower-shaped hydrogel composed of a bilayer lattice with a 90°/0° configuration was printed. Due to the anisotropic swelling, the petals closed when immersed in water. Similarly, when petals with the ink filaments oriented at −45°/45° were printed, twisted deformation was achieved. Not only oriented structures, but also bilayer structures, can be prepared by 3D printing and provide programmable deformation. Yum and coworkers printed a bilayer hydrogel actuator with a temperature-unresponsive poly(ethylene glycol) (PEG) layer and a temperature-responsive poly(N-isopropylacrylamide) (PNIPAm) layer (Fig. 9d).[84] The PEG layer restricted the isotropic deswelling behavior of the PNIPAm layer, allowing the flat bilayer hydrogel to transform into a saddle shape. Moreover, inspired by the morphology of bauhinia seed pods, both the PEG layer and the PNIPAm layer could be programmed with different orthogonally oriented layers at different angles to produce various complex morphologies such as linear contraction, bending, and twisting (Fig. 9e). 3D printing has created infinite possibilities for the preparation of anisotropic hydrogels, and it is anticipated that various shape transformation behaviors could be achieved *via* further combinations of 3D printing and shape deformation hydrogels.

5. Combined shape memory and actuating behavior

Although both the shape memory and actuation strategies provide programmable deformation, some major challenges remain. For example, shape memory hydrogels can be programmed into various temporary shapes, but cannot provide reversible transformation between the temporary shape and the permanent shape. Actuating hydrogels can exhibit reversible transformation behavior, but their deformation behavior cannot be altered due to their unchangeable anisotropic structure. The combination of shape memory and actuation behavior in a single system is an effective way to utilize the advantages of both strategies, and could achieve novel shape deformation behavior, which would be beneficial for applications in various fields.

5.1 Macro-anisotropy structures

In all types of anisotropic structures, hydrogel actuators with a bilayer structure usually contain two non-interfering layers; therefore, it is convenient to incorporate shape memory and actuation behavior into a bilayer hydrogel *via* different layers. In our previous work, a bilayer hydrogel actuator with a pH-responsive poly(acrylamide)-chitosan (PAAm-CS) layer (memorizing layer) and a thermo-responsive PNIPAm layer (actuating layer) was prepared *via* step-by-step photo-polymerization.[87] Unlike a traditional shape memorizing hydrogel, the bilayer hydrogel could automatically deform into a temporary shape and be fixed into the deformed shape under an external stimulus. For example, a bilayer hydrogel strip could be bent into a circle in response to a heat stimulus due to the hydrophilic–hydrophobic transition of PNIPAm, and the deformed circular shape could be memorized under alkaline conditions *via* the micro-crystallization of chitosan chains. Furthermore, various complex temporary shapes could be triggered by heat in the absence of an external manual force; this predetermined shape-shifting behavior provides a novel strategy to construct advanced shape-deforming hydrogels based on the combination of shape memory and actuation behavior.

Based on the above exploration, recently, we have developed a novel bilayer hydrogel with a thermoresponsive actuating layer (PNIPAm) and a metal-ion-responsive memorizing layer (alginate/polyacrylamide (Alg/PAAm)) (Fig. 10a).[88] Unlike in the case of traditional hydrogel actuators, in this system, temporary anisotropic structures could be formed and programmed using shape memory, and various morphing transformations could be induced by the actuating process. For instance, the wings of a butterfly-shaped bilayer hydrogel could first be fixed into a curved shape by metal ion–Alg interactions, and the wings could then deform from the curved shape into a soaring shape in response to a heat stimulus. In addition, assisted by kirigami (Fig. 10b), a 2D hydrogel sheet with deliberately cut patterns was rolled into a cylinder and both ends of it were treated with Fe^{3+}. The cylindrical hydrogel could then self-deform into a lantern in 60 °C water (Fig. 10c). Additionally, the hydrogel sheet was manually deformed into an arched shape, and the arched part was fixed using Fe^{3+}. Based on the shrinking of both ends of the
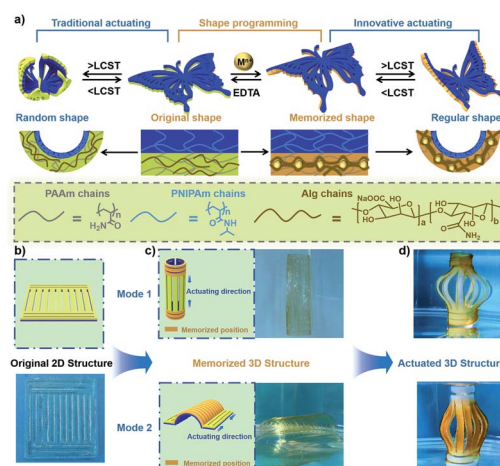

Fig. 10 (a) Schematic illustration of the traditional deformation process in programmable shape deformation generated by the combination of shape memory and actuation behavior. (b) Schematic illustration of the bilayer structure and the mechanism of shape memory and the actuation process. (c and d) Programmable deformation of a 2D sheet into a 3D lantern shape by the assistance of kirigami. Scale bars: 1 cm. Reproduced with permission from ref. 88. Copyright 2020 Wiley-VCH.

arched shape with increasing temperature, the lantern shape was achieved again. In this work, transient anisotropic structures were achieved using shape memory, and one hydrogel actuator could generate various programmable deformations, enabling innovative ideas for the design and fabrication of bioactuators.

5.2 Micro-anisotropy structures

Anisotropic structures can not only be changed at the macro level by the shape memory process, but can also be changed at the micro-scale, *e.g.*, molecular clusters. For example, Pan and coworkers prepared an isotropic hydrogel *via* the copolymerization of stearyl acrylate (SA) and PNIPAm and realized programmable deformation.[89] The melting transition of the stearyl segments is well known for both cooling-induced shape fixing and heating-induced recovery. Due to the hydrophobic interactions of the stearyl segments, when the original isotropic hydrogel was programmed using an external force and immersed in hot water, the PNIPAm chains collapsed and aggregated around the stearyl domains. Thus, the deformed shape could be fixed and transient structural anisotropy was achieved. When the hydrogel was placed in cool water again, although the macroscopic shape was recovered to the original state, the micro-structure was still anisotropic. Therefore, the hydrogel could self-deform into the temporary shape upon heating (Fig. 11a). This programmability allowed the hydrogels to reversibly shift between various shapes. For example, an isotropic pentagram-shaped hydrogel was folded into a pentagon shape and immersed in 45 °C water. The hydrogel could recover the original shape in 15 °C water and actuate to the temporary shape in 45 °C water (Fig. 11b). It is worth noting that the anisotropic structure can recover to the isotropic structure when the hydrogel is immersed in cool water for a long time. For instance, as shown in Fig. 11c, a hydrogel strip was programmed into an "Ω" shape and exhibited reversible transformation between the strip and "Ω" shapes. When the "Ω"-shaped hydrogel was immersed in cool water for 3 h, both the macro-shape and micro-structure recovered to the original state with an isotropic structure. The hydrogel strip could then be reprogrammed into a spiral shape and exhibited a reversible transformation between the strip and the spiral shape. This work innovatively combined shape memory and actuating behavior, and provided programmable reversible shape transformation between a temporary shape and a permanent shape, which may significantly expand the scope for designing future smart hydrogel-based devices.

6. Promising applications of shape deformation hydrogels

As mentioned above, shape deformation hydrogels could provide programmable deformation behavior tailored to a particular application scenario *via* the shape memorization and actuation processes. In the past years, shape deformation hydrogels have been designed and applied as grippers, artificial muscles, and walkers to realize the corresponding functions,
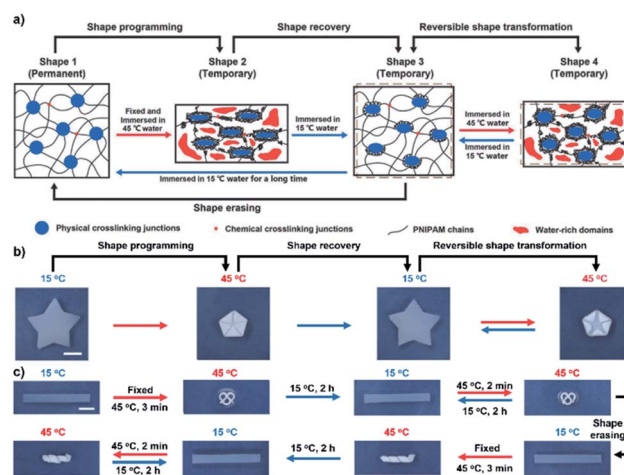

Fig. 11 (a) Schematic illustration showing a proposed mechanism for the programmable deformation behavior. (b) Images showing reversible shape deformation with an origami star, kirigami array, and randomly kneaded sheet. (c) Images showing reprogramming of a reversible shape transformation. Scale bars: 1 cm. Reproduced with permission from ref. 89. Copyright 2020 Wiley–VCH.

i.e., grasping, lifting and walking. Recently, increasing attention has been paid to the development of multifunctional shape deformation hydrogels and the exploration of their potential applications as soft robots, biomimetic devices, and information storage materials. In this section, we will discuss some novel design strategies and introduce the recent applications of shape deformation hydrogels.

6.1 Soft robots

Currently, almost all applications depend on the *in situ* deformation of the hydrogel. In fact, even simple bending actions can be transformed into walking, jumping or swimming behavior by applying a programmable cyclical stimulus.[51,90–92] For example, using a digital light processing (DLP) based micro-3D printing technique, Lee and coworkers prepared a humanoid 3D robot from electroactive hydrogels (EAH) that could exhibit a bending action in an electric field.[90] Through programmatically controlling the electric field, the body, legs, and arms of the robot could provide orchestrated bending actuation, which induced a sustained change of the center of gravity and kept the robot walking continuously. In addition to cyclic external stimuli, a constant external stimulus can also be applied to generate movement. Recently, He and coworkers embedded gold nanoparticles (AuNPs) in a PNIPAm hydrogel pillar and prepared a novel light-driven hydrogel oscillator (Fig. 12a).[93] As shown in Fig. 12b and c, when an arbitrary spot on the pillar was irradiated with a light source, the temperature of the illuminated area quickly increased above the volume phase transition temperature (VPTT) of PNIPAm. The pillar rapidly shrank, leading to the overbending state. The overbent tip blocked the light source, thus inducing the shape recovery process. During the shape recovery process, the hinge was again exposed to light, beginning the next cycle. Based on the powerful oscillator,
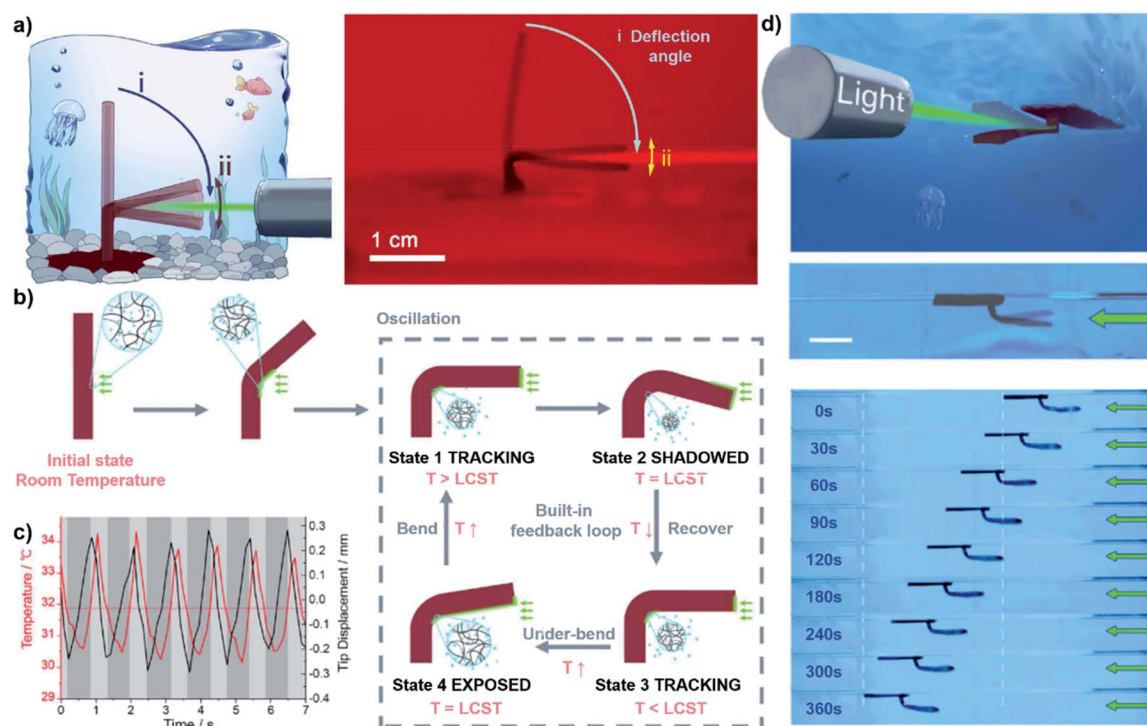
Fig. 12 (a) Schematic and image of the oscillating hydrogel. (b) Mechanism of the oscillation. (c) Time–resolved tip displacement and temperature of the hinge. (d) Schematic and images showing the swimming process of the oscillating hydrogel. Scale bars: 1 cm. Reproduced with permission from ref. 93. Copyright 2019 AAAS.

a phototaxis swimming robot was fabricated. As shown in Fig. 12d, a long hydrogel strip was employed as a paddle and attached perpendicular to a planar hydrogel sheet. When the paddle was irradiated by a light source, it continuously oscillated and provided the force for the robot to swim away. This system could potentially be used to generate a hydrogel motor and make soft robots more intelligent.

In a recent work, we proposed novel remotely controlled soft robots based on a shape memory hydrogel system. Fe_3O_4 magnetic nanoparticles were introduced into a double network structure with a chemically crosslinked poly(*N*-(2-hydroxyethyl) acrylamide) (PHEAA) and a reversibly crosslinked gelatin network.[94] As shown in Fig. 13a, when the double network hydrogel (HG-Fe_3O_4) was exposed to near-infrared light (NIR), the temperature of the hydrogel increased due to the photo-thermal heating of the Fe_3O_4 magnetic nanoparticles (Fig. 13b). With the rise in temperature, the triple helix structure of the gelatin network was untwisted into single coils (Fig. 13c), which caused both the cross-linking density and modulus of the HG-Fe_3O_4 hydrogel to decrease, making the HG-Fe_3O_4 hydrogel easier to deform under a magnetic field. Then, when the NIR was turned off, the temperature of HG-Fe_3O_4 hydrogel dropped to room temperature and the triple helix structure of gelatin was reconstructed, fixing the deformed shape. When the NIR was turned on again, the HG-Fe_3O_4 hydrogel could transform to the original shape spontaneously. As shown in Fig. 13d and e, the constructed three-pawed robot was too large to pass through the narrow channels of a maze. However, the robot could be

transformed into a folded shape with the assistance of NIR light and a magnetic field and then passed through the maze under the guidance of a magnet. After reaching a wider area, the folded robot could unfold and recover to the original shape remotely under NIR irradiation. This work may inspire the fabrication of intelligent soft robots based on shape deformation hydrogels.

6.2 Biomimetic devices

Nature is a source of inspiration for both the design and application of new materials. Recently, an increasing number of bio-inspired materials have been fabricated and exhibit simulated biological behavior.[95] Since they have a similar modulus to living tissues, stimuli-responsive hydrogels have been regarded as a highly anticipated bionic material to imitate biological behavior such as deformation, discoloration and movement. For example, a fluorescent hydrogel actuator could exhibit synergetic color-changing and 3D shape-morphing behavior similar to that of a chameleon.[55] Additionally, hydrogels can also exhibit self-growing behavior and become tougher, analogously to muscle training.[96] Inspired by octopus suckers, Liu and coworker developed an organohydrogel with a PAAm-*co*-PAAc hydrogel framework and microrganogel inclusions containing polystearyl methacrylate (PSMA) (Fig. 14a).[97] Due to the multistage phase transitions of the microrganogel inclusions, the organohydrogel exhibited stepwise switching mechanics and could be applied to prepare biomimetic soft suckers (Fig. 14b). In order to control the mechanical state of the
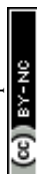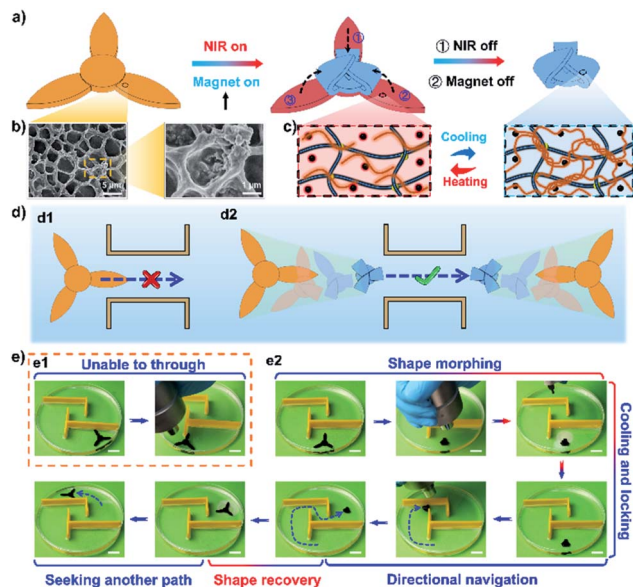
Fig. 13 (a) Schematic illustration showing the deformation process. The hydrogel is deformed by a magnetic field and the temporary shape is fixed under NIR irradiation; the hydrogel could subsequently be recovered to the original shape *via* an NIR stimulus. (b) SEM images of the Fe₃O₄ magnetic nanoparticles. (c) Shape memory mechanism of the gelatin-containing hydrogel. The hydrogel with single gelatin coils is deformed at high temperature, and the temporary shape is fixed when the untwisted chains are reconstructed at low temperature. (d) Schematic illustration showing the three-pawed robot passing through obstacles. (d1) The three-pawed robot is too large to pass through the narrow channels. (d2) The three-pawed robot can pass through the narrow channels after deforming into a folded shape. (e) Images showing the process of the robot passing through the maze with the help of NIR and an external magnetic field. Scale bars: 2 cm. Reproduced with permission from ref. 94. Copyright 2020 Wiley-VCH.

suckers *via* analog electrical stimuli, a polypyrrole (PPy) network was introduced into the organohydrogel system. As shown in Fig. 14c, a tough sucker failed to stick to a rough surface due to its inferior interface contact force. The novel suckers could decrease their modulus under an electrical stimulus of 8 V due to the thermoelectric effect of PPy, and improved their surface adaptability in order to conform with rough surfaces. When the electrical stimulus was turned off, the temporary shape was fixed *via* the crystallization of PSMA. Thus, the rough surface could be stuck and lifted firmly. Additionally, the organohydrogel also exhibited programmable surface topography and could be applied for unidirectional liquid transport inspired by the peristome surfaces of pitcher plants and the grooved surfaces of rice leaves (Fig. 14d).[98] The original smooth surface of the organohydrogels was encoded by a specific inverse mode at a temperature above T_m, and the corresponding surface morphology could be memorized by the formation of crystals upon reducing the temperature. As shown in Fig. 14e, liquid could be unidirectionally transported along two paths. When a path was irradiated by NIR, it was programmably closed *via* the shape recovery process. Therefore, the liquid could be transported along the elected path. These successful attempts

could expand the potential applications of smart biomimetic hydrogel devices.

6.3 3D encryption and decryption

In modern times, the storage and encryption of information have become highly important because of the huge damage that could be caused by information leakage.[99] Shape deformation hydrogels that can generate movement in response to certain external stimuli have been regarded as an emerging information storage material.[100] Recently, shape deformation hydrogels with incorporated fluorescent behavior[101,102] that provide multidimensional information encryption have been developed. For example, we demonstrated a fluorescent-hydrogel-based 3D anti-counterfeiting platform, which was fabricated by mixing a fluorescent macromolecule, perylene-tetracarboxylic-acid-modified gelatin (PTG), into poly(vinyl alcohol) (PVA) hydrogels (Fig. 15a).[103] The fluorescent hydrogel exhibited visible Fe^{3+}-controlled fluorescence quenching and borax-triggered shape memory behavior. As shown in Fig. 15b, the five petals of a 2D hydrogel were first manually deformed into a 3D hydrogel bowl. The temporary shape was then fixed by treatment with a borax solution to trigger a simultaneous shape memory process. Moreover, controllable fluorescence quenching behavior could be introduced into the shape memory process. As shown in Fig. 15c, Fe^{3+} was applied as an ink to write information, such as the letters "UCAS", onto the surface of a 2D hydrogel film. The hydrogel film was then folded into a 3D tetrahedron shape and immersed in borax solution in order to fix the temporary shape. It is obvious that the data "UCAS" cannot be recognized under either UV or visible light illumination. In a similar vein, the data "Q1A2Z3" was encrypted inside a 3D cube-shaped hydrogel origami structure. Due to the various ways of unfolding the cube, if a "spy" unfolds the cube in a wrong way, such as using external force, incorrect information would be presented and the correct information may remain hidden. Furthermore, a more complex 3D crane shape was developed in the same way, and a superior data security level was realized. Based on the exploration discussed above, we recently introduced the aggregation-induced-emissive monomer (4-(dimethylamino) ethoxy-*N*-allyl-1,8-naphthalimide, DAEAN) into a hydrogel network and prepared a poly(AAc-*co*-AAm-*co*-DAEAN) hydrogel with thermo-triggered multistate fluorescence switching behavior based on shape memory.[104]

Not only shape memory, but also programmable actuating processes, can be incorporated with fluorescence properties to achieve information encryption. In our previous work, a fluorescent monomer, 1-pyrenylmethyl acrylate (PyMA), was introduced into a PAAm-*co*-PAAc hydrogel network and emitted blue fluorescence under ultraviolet light. Through ionoprinting, a dried filter containing Fe^{3+} was placed in direct contact with the hydrogel.[105] The intramolecular charge transfer (ICT) between pyrene and Fe^{3+} quenched the fluorescence of the hydrogel. Thus, a blank hydrogel was loaded with the required information, which could only be recognized under ultraviolet light. Additionally, Fe^{3+} increased the local cross-linking of the PAAm-*co*-PAAc hydrogel, causing the finger of a hand-shaped
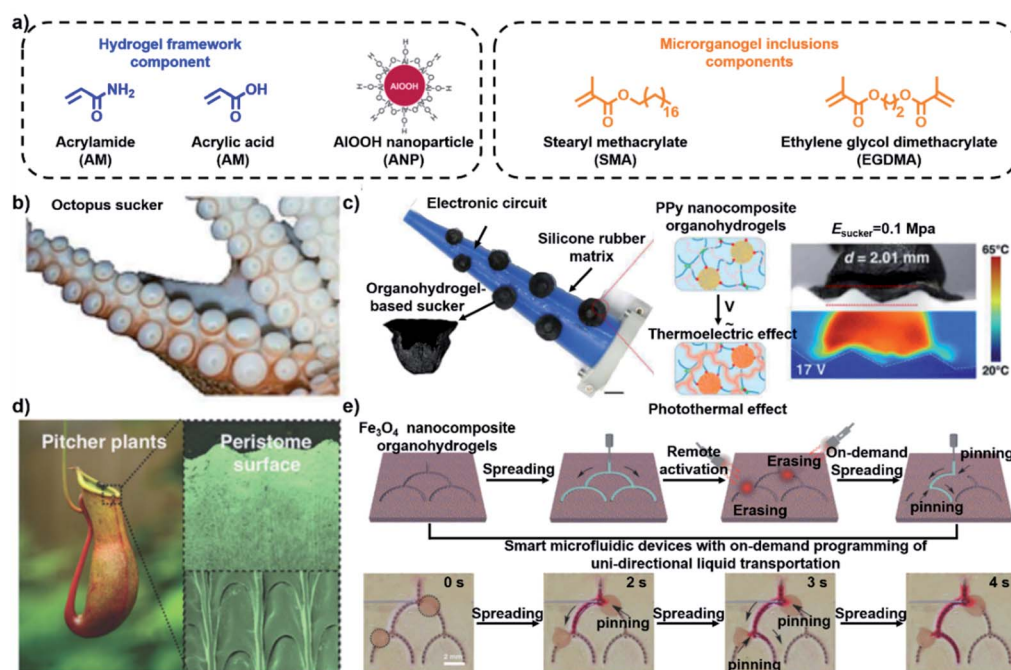
Fig. 14 (a) Chemical structure of the organohydrogel. (b) Image of octopus suckers. (c) Images showing the programmable adaptability of a bionomic tentacle. Scale bars: 1 cm. Reproduced with permission from ref. 97. Copyright 2020 AAAS. (d) Images of the surface of pitcher plants. (e) Schematic and images showing the process of unidirectional liquid transport. Scale bars: 2 mm. Reproduced with permission from ref. 98. Copyright 2019 Wiley-VCH.
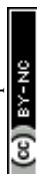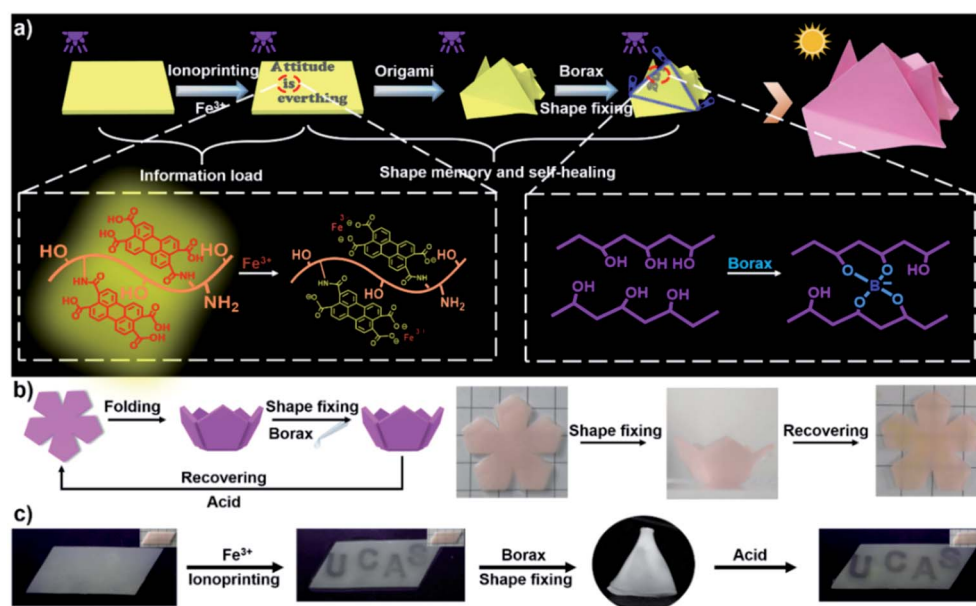

Fig. 15 (a) Schematic illustration showing the information encryption and decryption processes of the fluorescent hydrogel. (b) Schematic and images showing the shape memory process. (c) 3D information encryption and decryption processes: the information is loaded onto a 2D hydrogel sheet and encrypted inside a 3D hydrogel geometry during the shape memory process. Reproduced with permission from ref. 103. Copyright 2019 Wiley-VCH.

hydrogel to bend in water and exhibit various gesture information. Therefore, step-by-step information decryption could be achieved by introducing UV and water stimuli in a stepwise manner.

7. Summary and outlook

In this review, we have presented a comprehensive summary of the latest progress in programmable deformation hydrogels,

including shape memory hydrogels, actuating hydrogels, and hydrogels that combine shape memory and actuation. Moreover, some successful explorations of soft robot, biomimetic device, and information encryption applications have been introduced. However, in addition to programmable shape deformation, an intelligent robot system should be practical, with better environmental adaptability, durability, and repeatability. Therefore, despite the aforementioned major achievements in shape deformation hydrogels, challenges and opportunities remain that must be addressed in future research work.

First of all, although many effective strategies to prepare hydrogels with excellent mechanical properties have been proposed, it is still challenging to fabricate shape deformation hydrogels with a high modulus. This is because the trade-off between the modulus and deformability of a hydrogel is difficult to balance. For example, the higher the modulus a hydrogel has, the tougher it is, and the actuating force may be too slight to actuate a tough hydrogel. Improving the mechanical properties of a deformation hydrogel will allow soft grippers to grasp heavier objects and artificial muscles to lift more objects, which will expand the practical applications of soft robots.

Second, the recently developed shape deformation hydrogels may face great challenges in real life. For instance, shape deformation hydrogels may lose water in a dry environment, over-swell in a wet environment or even be frozen in a cold environment; these negative conditions may interfere with their deformation properties. Recently, some successful strategies have been explored to fabricate hydrogels with excellent environmental stability, and most of the methods mentioned above to fabricate shape deformation hydrogels are universal methods. It is anticipated that the methods of fabricating shape deformation hydrogels could be combined with the methods of fabricating environmentally stable hydrogels without interference. Therefore, with appropriate selection and careful design, we should be able to fabricate multi-functional shape deformation hydrogels in the near future.

Third, at the present stage, deformable hydrogels exhibit only two states: the original and the final state. In practical applications, controlling the hydrogel to stay in a certain state during the deformation process will make it more useful. To achieve this goal, novel molecular design strategies should be explored to achieve shape deformation hydrogels with multiple stable states.

Fourth, through novel designs, even simple deformations can be used to evoke motion behaviors such as walking and oscillation. Thus, the macroscopic structure of deformable hydrogels should be designed to endow the hydrogels with more motion behavior, such as jumping and running. Moreover, deformation could be combined with motion, which could make the hydrogel robots more functional and able to overcome the obstacles on the way.

Last but not least, shape deformation hydrogels with sensing abilities, which would allow hydrogel robots to feed back their movement *via* other means such as electrical signals, should be explored and demonstrated in the future. In order to overcome the challenges mentioned above, many factors, such as shape

deformation mechanisms, mechanical properties, and application scenarios, should be investigated further in order to bring shape deformation hydrogels into practical real-world application.

Author contributions

Baoyi Wu contributed to conceptualization, data curation, formal analysis, visualization, writing-original draft. Jiawei Zhang contributed to validation and writing-review & editing. Huanhuan Lu contributed to part of visualization. Xiaoxia Le and Wei Lu contributed to conceptualization. Jiawei Zhang, Patrick Théato and Tao Chen conceived and designed the project. All authors read and approved the final manuscript.

Conflicts of interest

The authors declare no conflict of interest.

Acknowledgements

References

1 H. Fan and J. P. Gong, *Macromolecules*, 2020, **53**, 2769–2782.
2 M. Liu, S. Wang and L. Jiang, *Nat. Rev. Mater.*, 2017, **2**, 17036–17053.
3 L. Sun, Y. Yu, Z. Chen, F. Bian, F. Ye, L. Sun and Y. Zhao, *Chem. Soc. Rev.*, 2020, **49**, 4043–4069.
4 X. L. Gong, Y. Y. Xiao, M. Pan, Y. Kang, B. J. Li and S. Zhang, *ACS Appl. Mater. Interfaces*, 2016, **8**, 27432–27437.
5 X. Le, W. Lu, H. Xiao, L. Wang, C. Ma, J. Zhang, Y. Huang and T. Chen, *ACS Appl. Mater. Interfaces*, 2017, **9**, 9038–9044.
6 R. Li, D. Jin, D. Pan, S. Ji, C. Xin, G. Liu, S. Fan, H. Wu, J. Li, Y. Hu, D. Wu, L. Zhang and J. Chu, *ACS Nano*, 2020, **14**, 5233–5242.
7 M. Hua, D. Wu, S. Wu, Y. Ma, Y. Alsaid and X. He, *ACS Appl. Mater. Interfaces*, 2020, DOI: 10.1021/acsami.0c17532.
8 L. Hua, M. Xie, Y. Jian, B. Wu, C. Chen and C. Zhao, *ACS Appl. Mater. Interfaces*, 2019, **11**, 43641–43648.
9 Z. J. Wang, C. Y. Li, X. Y. Zhao, Z. L. Wu and Q. Zheng, *J. Mater. Chem. B*, 2019, **7**, 1674–1678.
10 C. Ma, X. Le, X. Tang, J. He, P. Xiao, J. Zheng, H. Xiao, W. Lu, J. Zhang, Y. Huang and T. Chen, *Adv. Funct. Mater.*, 2016, **26**, 8670–8676.
11 S. Xiao, M. Zhang, X. He, L. Huang, Y. Zhang, B. Ren, M. Zhong, Y. Chang, J. Yang and J. Zheng, *ACS Appl. Mater. Interfaces*, 2018, **10**, 21642–21653.

12 H. Cui, N. Pan, W. Fan, C. Liu, Y. Li, Y. Xia and K. Sui, *Adv. Funct. Mater.*, 2019, **29**, 1807692.

13 C. Li, A. Iscen, H. Sai, K. Sato, N. A. Sather, S. M. Chin, Z. Alvarez, L. C. Palmer, G. C. Schatz and S. I. Stupp, *Nat. Mater.*, 2020, **19**, 900–909.

14 C. Li, A. Iscen, L. C. Palmer, G. C. Schatz and S. I. Stupp, *J. Am. Chem. Soc.*, 2020, **142**, 8447–8453.

15 H. Guo, Q. Zhang, W. Liu and Z. Nie, *ACS Appl. Mater. Interfaces*, 2020, **12**, 13521–13528.

16 A. Lendlein and O. E. C. Gould, *Nat. Rev. Mater.*, 2019, **4**, 116–133.

17 A. S. Kuenstler, H. Kim and R. C. Hayward, *Adv. Mater.*, 2019, **31**, 1901216.

18 L. Ionov, *Adv. Funct. Mater.*, 2013, **23**, 4555–4570.

19 H. Ko and A. Javey, *Acc. Chem. Res.*, 2017, **50**, 691–702.

20 X. Du, H. Cui, T. Xu, C. Huang, Y. Wang, Q. Zhao, Y. Xu and X. Wu, *Adv. Funct. Mater.*, 2020, **30**, 1909202.

21 Q. L. Zhu, C. Du, Y. Dai, M. Daab, M. Matejdes, J. Breu, W. Hong, Q. Zheng and Z. L. Wu, *Nat. Commun.*, 2020, **11**, 5166–5177.

22 Y. Cheng, K. H. Chan, X. Q. Wang, T. Ding, T. Li, X. Lu and G. W. Ho, *ACS Nano*, 2019, **13**, 13176–13184.

23 M. Baumgartner, F. Hartmann, M. Drack, D. Preninger, D. Wirthl, R. Gerstmayr, L. Lehner, G. Mao, R. Pruckner, S. Demchyshyn, L. Reiter, M. Strobel, T. Stockinger, D. Schiller, S. Kimeswenger, F. Greibich, G. Buchberger, E. Bradt, S. Hild, S. Bauer and M. Kaltenbrunner, *Nat. Mater.*, 2020, **19**, 1102–1109.

24 Q. Yu, J. M. Bauer, J. S. Moore and D. J. Beebe, *Appl. Phys. Lett.*, 2001, **78**, 2589–2591.

25 Y. Jian, B. Wu, X. Le, Y. Liang, Y. Zhang, D. Zhang, L. Zhang, W. Lu, J. Zhang and T. Chen, *Research*, 2019, **2019**, 2384347.

26 Y. Zhang, J. Liao, T. Wang, W. Sun and Z. Tong, *Adv. Funct. Mater.*, 2018, **28**, 1707245.

27 Z. Zhao, S. Zhuo, R. Fang, L. Zhang, X. Zhou, Y. Xu, J. Zhang, Z. Dong, L. Jiang and M. Liu, *Adv. Mater.*, 2018, **30**, 1804435.

28 S. Huang, X. Xia, R. Fan and Z. Qian, *Chem. Mater.*, 2020, **32**, 1937–1945.

29 J. Li, Q. Ma, Y. Xu, M. Yang, Q. Wu, F. Wang and P. Sun, *ACS Appl. Mater. Interfaces*, 2020, **12**, 55290–55298.

30 C. Ma, W. Lu, X. Yang, J. He, X. Le, L. Wang, J. Zhang, M. J. Serpe, Y. Huang and T. Chen, *Adv. Funct. Mater.*, 2018, **28**, 1704568.

31 W. Lu, X. Le, J. Zhang, Y. Huang and T. Chen, *Chem. Soc. Rev.*, 2017, **46**, 1284–1294.

32 X. Le, W. Lu, J. Zhang and T. Chen, *Adv. Sci.*, 2019, **6**, 1801584.

33 C. Lowenberg, M. Balk, C. Wischke, M. Behl and A. Lendlein, *Acc. Chem. Res.*, 2017, **50**, 723–732.

34 R. Kempaiah and Z. Nie, *J. Mater. Chem. B*, 2014, **2**, 2357–2368.

35 Y. Osada and A. Matsuda, *Nature*, 1995, **376**, 219.

36 Z. Li, G. Davidson-Rozenfeld, M. Vazquez-Gonzalez, M. Fadeev, J. Zhang, H. Tian and I. Willner, *J. Am. Chem. Soc.*, 2018, **140**, 17691–17701.

37 B. Xu, Y. Zhang and W. Liu, *Macromol. Rapid Commun.*, 2015, **36**, 1585–1591.

38 H. Meng, P. Xiao, J. Gu, X. Wen, J. Xu, C. Zhao, J. Zhang and T. Chen, *Chem. Commun.*, 2014, **50**, 12277–12280.

39 X. Le, W. Lu, J. Zheng, D. Tong, N. Zhao, C. Ma, H. Xiao, J. Zhang, Y. Huang and T. Chen, *Chem. Sci.*, 2016, **7**, 6715–6720.

40 K. Miyamae, M. Nakahata, Y. Takashima and A. Harada, *Angew. Chem., Int. Ed.*, 2015, **54**, 8984–8987.

41 Z. Q. Dong, Y. Cao, Q. J. Yuan, Y. F. Wang, J. H. Li, B. J. Li and S. Zhang, *Macromol. Rapid Commun.*, 2013, **34**, 867–872.

42 H. Meng, J. Zheng, X. Wen, Z. Cai, J. Zhang and T. Chen, *Macromol. Rapid Commun.*, 2015, **36**, 533–537.

43 Z. Li, W. Lu, T. Ngai, X. Le, J. Zheng, N. Zhao, Y. Huang, X. Wen, J. Zhang and T. Chen, *Polym. Chem.*, 2016, **7**, 5343–5346.

44 J. Zheng, P. Xiao, X. Le, W. Lu, P. Théato, C. Ma, B. Du, J. Zhang, Y. Huang and T. Chen, *J. Mater. Chem. C*, 2018, **6**, 1320–1327.

45 X. He, Y. Sun, J. Wu, Y. Wang, F. Chen, P. Fan, M. Zhong, S. Xiao, D. Zhang, J. Yang and J. Zheng, *J. Mater. Chem. C*, 2019, **7**, 4970–4980.

46 R. Luo, J. Wu, N. Dinh and C. Chen, *Adv. Funct. Mater.*, 2015, **25**, 7272–7279.

47 W. Fan, C. Shan, H. Guo, J. Sang, R. Wang, R. Zheng, K. Sui and Z. Nie, *Sci. Adv.*, 2019, **5**, eaav7174.

48 B. Y. Wu, X. X. Le, Y. K. Jian, W. Lu, Z. Y. Yang, Z. K. Zheng, P. Theato, J. W. Zhang, A. Zhang and T. Chen, *Macromol. Rapid Commun.*, 2019, **40**, 1800648.

49 Z. L. Wu, M. Moshe, J. Greener, H. Therien-Aubin, Z. Nie, E. Sharon and E. Kumacheva, *Nat. Commun.*, 2013, **4**, 1586–1593.

50 H. Therien-Aubin, Z. L. Wu, Z. Nie and E. Kumacheva, *J. Am. Chem. Soc.*, 2013, **135**, 4834–4839.

51 Y. S. Kim, M. Liu, Y. Ishida, Y. Ebina, M. Osada, T. Sasaki, T. Hikima, M. Takata and T. Aida, *Nat. Mater.*, 2015, **14**, 1002–1007.

52 Z. Sun, Y. Yamauchi, F. Araoka, Y. S. Kim, J. Bergueiro, Y. Ishida, Y. Ebina, T. Sasaki, T. Hikima and T. Aida, *Angew. Chem., Int. Ed.*, 2018, **57**, 15772–15776.

53 A. M. Hubbard, W. Cui, Y. Huang, R. Takahashi, M. D. Dickey, J. Genzer, D. R. King and J. P. Gong, *Matter*, 2019, **1**, 674–689.

54 H. Lin, S. Ma, B. Yu, X. Pei, M. Cai, Z. Zheng, F. Zhou and W. Liu, *Chem. Mater.*, 2019, **31**, 9504–9512.

55 S. Wei, W. Lu, X. Le, C. Ma, H. Lin, B. Wu, J. Zhang, P. Theato and T. Chen, *Angew. Chem., Int. Ed.*, 2019, **58**, 16243–16251.

56 D. Han, C. Farino, C. Yang, T. Scott, D. Browe, W. Choi, J. W. Freeman and H. Lee, *ACS Appl. Mater. Interfaces*, 2018, **10**, 17512–17518.

57 S. R. Goudu, I. C. Yasa, X. Hu, H. Ceylan, W. Hu and M. Sitti, *Adv. Funct. Mater.*, 2020, **30**, 2004975.

58 C. F. Dai, C. Du, Y. Xue, X. N. Zhang, S. Y. Zheng, K. Liu, Z. L. Wu and Q. Zheng, *ACS Appl. Mater. Interfaces*, 2019, **11**, 43631–43640.

59 S. Wang, S. Li and L. Gao, *ACS Appl. Mater. Interfaces*, 2019, **11**, 43622–43630.
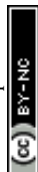
60 H. Xiao, W. Lu, X. Le, C. Ma, Z. Li, J. Zheng, J. Zhang, Y. Huang and T. Chen, *Chem. Commun.*, 2016, **52**, 13292–13295.

61 Z. Zhao, K. Zhang, Y. Liu, J. Zhou and M. Liu, *Adv. Mater.*, 2017, **29**, 1701695.

62 Z. Zhao, Y. Liu, K. Zhang, S. Zhuo, R. Fang, J. Zhang, L. Jiang and M. Liu, *Angew. Chem., Int. Ed.*, 2017, **56**, 13464–13469.

63 H. Xiao, C. Ma, X. Le, L. Wang, W. Lu, P. Theato, T. Hu, J. Zhang and T. Chen, *Polymers*, 2017, **9**, 138–148.

64 Z. Jiang, B. Diggle, I. C. G. Shackleford and L. A. Connal, *Adv. Mater.*, 2019, **31**, 1904956.

65 Z. J. Wang, C. N. Zhu, W. Hong, Z. L. Wu and Q. Zheng, *Sci. Adv.*, 2017, **3**, e1700348.

66 Z. J. Wang, W. Hong, Z. L. Wu and Q. Zheng, *Angew. Chem., Int. Ed.*, 2017, **56**, 15974–15978.

67 L. Huang, R. Jiang, J. Wu, J. Song, H. Bai, B. Li, Q. Zhao and T. Xie, *Adv. Mater.*, 2017, **29**, 1605390.

68 A. Nojoomi, H. Arslan, K. Lee and K. Yum, *Nat. Commun.*, 2018, **9**, 3705–3716.

69 X. P. Hao, Z. Xu, C. Y. Li, W. Hong, Q. Zheng and Z. L. Wu, *Adv. Mater.*, 2020, **32**, 2000781.

70 M. Liu, Y. Ishida, Y. Ebina, T. Sasaki, T. Hikima, M. Takata and T. Aida, *Nature*, 2015, **517**, 68–72.

71 Q. L. Zhu, C. F. Dai, D. Wagner, M. Daab, W. Hong, J. Breu, Q. Zheng and Z. L. Wu, *Adv. Mater.*, 2020, **32**, 2005567.

72 C. Ma, T. Li, Q. Zhao, X. Yang, J. Wu, Y. Luo and T. Xie, *Adv. Mater.*, 2014, **26**, 5665–5669.

73 B. Wu, Y. Xu, X. Le, Y. Jian, W. Lu, J. Zhang and T. Chen, *Acta Polym. Sin.*, 2019, **50**, 496–504.

74 Z. Xu and J. Fu, *ACS Appl. Mater. Interfaces*, 2020, **12**, 26476–26484.

75 X. Peng, T. Liu, Q. Zhang, C. Shang, Q. W. Bai and H. Wang, *Adv. Funct. Mater.*, 2017, **27**, 1701962.

76 T. Li, J. Wang, L. Zhang, J. Yang, M. Yang, D. Zhu, X. Zhou, S. Handschuh-Wang, Y. Liu and X. Zhou, *J. Mater. Chem. B*, 2017, **5**, 5726–5732.

77 X. Du, H. Cui, Q. Zhao, J. Wang, H. Chen and Y. Wang, *Research*, 2019, **2019**, 1–12.

78 S. Hong, D. Sycks, H. F. Chan, S. Lin, G. P. Lopez, F. Guilak, K. W. Leong and X. Zhao, *Adv. Mater.*, 2015, **27**, 4035–4040.

79 Z. Chen, D. Zhao, B. Liu, G. Nian, X. Li, J. Yin, S. Qu and W. Yang, *Adv. Funct. Mater.*, 2019, **29**, 1900971.

80 F. Gao, Z. Xu, Q. Liang, B. Liu, H. Li, Y. Wu, Y. Zhang, Z. Lin, M. Wu, C. Ruan and W. Liu, *Adv. Funct. Mater.*, 2018, **28**, 1706644.

81 H. Zhang, Y. Cong, A. R. Osi, Y. Zhou, F. Huang, R. P. Zaccaria, J. Chen, R. Wang and J. Fu, *Adv. Funct. Mater.*, 2020, **30**, 1910573.

82 Y. Zhang, X. Yin, M. Zheng, C. Moorlag, J. Yang and Z. L. Wang, *J. Mater. Chem. A*, 2019, **7**, 6972–6984.

83 A. S. Gladman, E. A. Matsumoto, R. G. Nuzzo, L. Mahadevan and J. A. Lewis, *Nat. Mater.*, 2016, **15**, 413–418.

84 H. Arslan, A. Nojoomi, J. Jeon and K. Yum, *Adv. Sci.*, 2019, **6**, 1800703.

85 Y. Hu, Z. Wang, D. Jin, C. Zhang, R. Sun, Z. Li, K. Hu, J. Ni, Z. Cai, D. Pan, X. Wang, W. Zhu, J. Li, D. Wu, L. Zhang and J. Chu, *Adv. Funct. Mater.*, 2019, **30**, 1907377.

86 S. Y. Zheng, Y. Shen, F. Zhu, J. Yin, J. Qian, J. Fu, Z. L. Wu and Q. Zheng, *Adv. Funct. Mater.*, 2018, **28**, 1803366.

87 L. Wang, Y. Jian, X. Le, W. Lu, C. Ma, J. Zhang, Y. Huang, C. F. Huang and T. Chen, *Chem. Commun.*, 2018, **54**, 1229–1232.

88 H. Lu, B. Wu, X. Yang, J. Zhang, Y. Jian, H. Yan, D. Zhang, Q. Xue and T. Chen, *Small*, 2020, **16**, 2005461.

89 K. Liu, Y. Zhang, H. Cao, H. Liu, Y. Geng, W. Yuan, J. Zhou, Z. L. Wu, G. Shan, Y. Bao, Q. Zhao, T. Xie and P. Pan, *Adv. Mater.*, 2020, **32**, 2001693.

90 D. Han, C. Farino, C. Yang, T. Scott, D. Browe, W. Choi, J. W. Freeman and H. Lee, *ACS Appl. Mater. Interfaces*, 2018, **10**, 17512–17518.

91 G. Gao, Z. Wang, D. Xu, L. Wang, T. Xu, H. Zhang, J. Chen and J. Fu, *ACS Appl. Mater. Interfaces*, 2018, **10**, 41724–41731.

92 Q. Zhao, Y. Liang, L. Ren, Z. Yu, Z. Zhang and L. Ren, *Nano Energy*, 2018, **51**, 621–631.

93 Y. Zhao, X. Chen, X. Qian, Y. Alsaid, M. Hua, L. Jin and X. He, *Sci. Robot.*, 2019, **4**, eaax7112.

94 D. Zhang, J. Zhang, Y. Jian, B. Wu, H. Yan, H. Lu, S. Wei, S. Wu, Q. Xue and T. Chen, *Adv. Intell. Syst.*, 2020, DOI: 10.1002/aisy.202000208.

95 Y. Ma, M. Hua, S. Wu, Y. Du, X. Pei, X. Zhu, F. Zhou and X. He, *Sci. Adv.*, 2020, **6**, eabd2520.

96 T. Matsuda, R. Kawakami, R. Namba, T. Nakajima and J. P. Gong, *Science*, 2019, **363**, 504–508.

97 S. Zhuo, Z. Zhao, Z. Xie, Y. Hao, Y. Xu, T. Zhao, H. Li, E. M. Knubben, L. Wen, L. Jiang and M. Liu, *Sci. Adv.*, 2020, **6**, eaax1464.

98 Z. Zhao, C. Li, Z. Dong, Y. Yang, L. Zhang, S. Zhuo, X. Zhou, Y. Xu, L. Jiang and M. Liu, *Adv. Funct. Mater.*, 2019, **29**, 1807858.

99 X. Le, H. Shang, H. Yan, J. Zhang, W. Lu, M. Liu, L. Wang, G. Lu, Q. Xue and T. Chen, *Angew. Chem., Int. Ed.*, 2021, **60**, 3640–3646.

100 P. Li, D. Zhang, Y. Zhang, W. Lu, J. Zhang, W. Wang, Q. He, P. Théato and T. Chen, *ACS Macro Lett.*, 2019, **8**, 937–942.

101 W. Lu, C. Ma, D. Zhang, X. Le, J. Zhang, Y. Huang, C.-F. Huang and T. Chen, *J. Phys. Chem. C*, 2018, **122**, 9499–9506.

102 Y. K. Jian, X. X. Le, Y. C. Zhang, W. Lu, L. Wang, J. Zheng, J. W. Zhang, Y. J. Huang and T. Chen, *Macromol. Rapid Commun.*, 2018, **39**, 1800130.

103 Y. Zhang, X. Le, Y. Jian, W. Lu, J. Zhang and T. Chen, *Adv. Funct. Mater.*, 2019, **29**, 1905514.

104 H. Qiu, S. Wei, H. Liu, B. Zhan, H. Yan, W. Lu, J. Zhang, S. Wu and T. Chen, *Adv. Intell. Syst.*, 2021, DOI: 10.1002/aisy.202000239.

105 X. Le, W. Lu, J. He, M. J. Serpe, J. Zhang and T. Chen, *Sci. China Mater.*, 2018, **62**, 831–839.